Molecular Therapy
Oncolytics
Original Article

AMERICAN SOCIETY of GENE & CELL THERAPY

MAPK Inhibitors Enhance HDAC Inhibitor-Induced Redifferentiation in Papillary Thyroid Cancer Cells Harboring *BRAF*^{V600E}: An *In Vitro* Study

Hao Fu,[1,4] Lingxiao Cheng,[1,2,4] Yuchen Jin,[1] Lin Cheng,[1] Min Liu,[1,3] and Libo Chen[1]

[1]Department of Nuclear Medicine, Shanghai Jiao Tong University Affiliated Sixth People's Hospital, 600 Yishan Road, Shanghai 200233, China; [2]Department of Nuclear Medicine, Sir Run Run Shaw Hospital, School of Medicine, Zhejiang University, 3 Qingchun East Road, Hangzhou 310016, Zhejiang, China; [3]Department of Nuclear Medicine, Zhongshan Hospital, Fudan University, 180 Fenglin Road, Shanghai 200032, China

Clinical efficacy of redifferentiation therapy with histone deacetylase inhibitor (HDACi) for lethal radioiodine-refractory papillary thyroid cancer (RR-PTC) is urgently needed to be improved. Given that the impairment of histone acetylation is a mechanism in *BRAF*^{V600E}-mitogen-activated protein kinase (MAPK)-induced aberrant silencing of thyroid iodine-metabolizing genes, dual inhibition of HDAC and MAPK may produce a more favorable effect. In this study, we treated *BRAF*^{V600E}-mutant (BCPAP and K1) and *BRAF*-wild-type (BHP 2-7) cells with HDACi (panobinostat) and MAPK inhibitor (dabrafenib or selumetinib), alone or in combination, and we tested the expression of iodine- and glucose-metabolizing genes, radioiodine uptake and efflux, and toxicity. We found that panobinostat alone increased iodine-metabolizing gene expression, promoted radioiodine uptake and toxicity, and suppressed *GLUT1* expression in all the cells. However, MAPKi (dabrafenib or selumetinib) induced these effects only in *BRAF*^{V600E}-mutant cells. Combined treatment with panobinostat and MAPKi (dabrafenib or selumetinib) displayed a more robust *BRAF*^{V600E}-dependent redifferentiation effect than panobinostat alone via further improving the acetylation level of histone at the sodium-iodide symporter (*NIS*) promoter. In conclusion, MAPK inhibitors enhance HDACi-induced redifferentiation in PTC cells harboring *BRAF*^{V600E}, warranting animal and clinical trials.

INTRODUCTION

Radioiodine therapy is a conventional and effective treatment for differentiated thyroid cancer (DTC), which is based on the ability of thyroid follicular cells to concentrate radioiodine via the sodium-iodide symporter (NIS).[1,2] As previously reviewed by our team, in nearly half of the DTC patients with persistent or recurrent or metastatic lesions,[3] however, tumors go through a dedifferentiation process and lose the ability to take up radioiodine, which is named radioiodine-refractory DTC (RR-DTC).[4] A major mechanism underlying the development of RR-DTC is the aberrant silencing of iodine-metabolizing genes in thyroid cancer cells, such as *NIS*, thyroglobulin (*TG*), thyroid-stimulating hormone receptor (*TSHR*), and thyroperoxidase (*TPO*).[5] Furthermore, RR-DTC patients have a dismal prognosis, with an overall survival of 10% at 10 years.[6] Fluorodeoxyglucose (FDG)-avid lesions can be usually identified in such patients due to the overexpression of glucose transporter type 1 (*GLUT1*) gene.[5,7,8]

Histone acetylation at the promoter area is a well-established mechanism in the upregulation of gene expression, which, through chromatin remodeling, opens up the access of gene promoters to transcription factors. Conversely, histone deacetylation causes blocking of gene promoters from binding with the transcription factors, resulting in gene silencing.[9] Iodine-metabolizing gene silencing is also related to histone deacetylation, and histone deacetylation (HDAC) inhibitors could induce the expression of iodine-metabolizing genes and radioiodine uptake in thyroid cancer cells and even in certain nonthyroid epithelial cancer cells.[10–13] Additionally, HDAC inhibitors can also suppress the expression of *GLUT1*.[14] Unfortunately, clinical studies have demonstrated that inhibiting HDAC alone could only induce radioiodine uptake in RR-DTC patients, but therapeutic effect could not be achieved either used alone or in combination with radioiodine.[15,16]

Recently, iodine-metabolizing gene silencing in thyroid cancer has been revealed to be associated with aberrant activation of the mitogen-activated protein kinase (MAPK) pathway, which is frequently caused by the *BRAF*^{V600E} mutation.[7] Increasing evidence, including our previous study, has demonstrated that MAPK inhibitors and multikinase inhibitors can induce redifferentiation in thyroid cancer;[10,17,18] however, their clinical effectiveness to restore ^{131}I uptake remains insufficient.[19] Although the clinically tested MEK inhibitor selumetinib has shown promising redifferentiation efficacy, it unfortunately seemed to be most effective in thyroid cancers with an *NRAS* mutation, leaving the question of how to treat the more

Received 5 October 2018; accepted 28 January 2019;
https://doi.org/10.1016/j.omto.2019.01.007.

[4]These authors contributed equally to this work.

Correspondence: Libo Chen, MD, PhD, Department of Nuclear Medicine, Shanghai Jiao Tong University Affiliated Sixth People's Hospital, 600 Yishan Road, Shanghai 200233, China.
E-mail: lbchen@sjtu.edu.cn

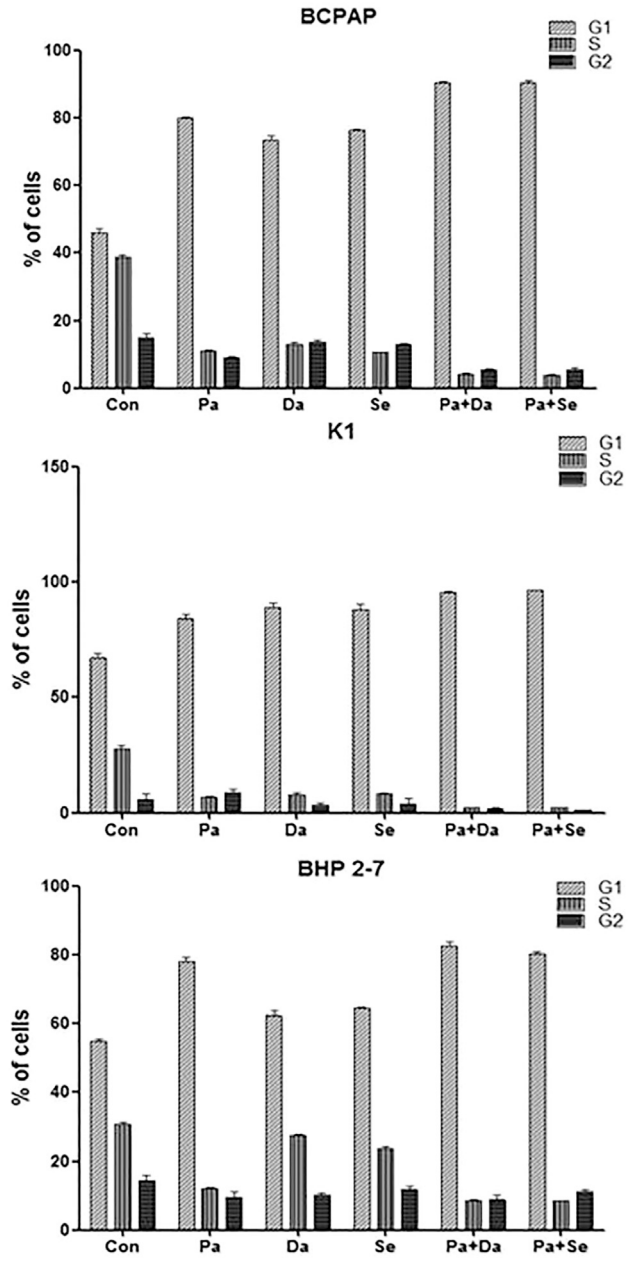

Figure 1. Cell Cycle of BCPAP, K1, and BHP2-7 Treated with 0.05 μM Panobinostat and 0.1 μM Dabrafenib/2.5 μM Selumetinib Individually, in Combination, or with DMSO for 24 h

In BCPAP and K1 cells treated with panobinostat or MAPKi (dabrafenib or selumetinib) alone, the proportion of G1-phase cells was more than that in the DMSO control group. More cells were arrested in G1 phase when cells were treated with panobinostat in combination with MAPKi (dabrafenib or selumetinib). The number of G1 cells in panobinostat-treated BHP 2-7 cells was more than that in DMSO control; proportions of G1 cells in MAPKi (dabrafenib or selumetinib)-treated BHP 2-7 cells were not significantly different from that in the DMSO control, and the number of G1 cells in the combined treatment group was not significantly different from that in the panobinostat-treated group.

commonly found $BRAF^{V600E}$ mutation that is associated with poor prognosis unanswered.[20] More recently, $BRAF^{V600E}$-specific inhibitor dabrafenib demonstrated new radioiodine uptake in 60% of 10 patients with $BRAF^{V600E}$-mutant iodine-refractory papillary thyroid cancer (PTC), but an objective response of only 20%.[21] It can be concluded that the redifferentiation effect of MAPK inhibitors, to date, also remains to be improved.

Inspiringly, it has been demonstrated that the MAPK pathway down-regulates histone acetylation in the important transcriptional factor-binding sites of iodine-metabolizing gene promoters, which ultimately causes the aberrant silencing of iodine-metabolizing genes in thyroid cancer.[22] The *NIS* promoter is most commonly affected by $BRAF^{V600E}$ mutation-triggered HDAC, resulting in silencing of the *NIS* gene. We, therefore, hypothesize that simultaneously inhibiting HDAC and the MAPK pathway may yield a synergistic effect on thyroid-specific gene expression and radioiodine uptake in thyroid cancer cells. In this study, we tested whether the simultaneous inhibition of HDAC and the MAPK pathway can induce a more intense redifferentiation effect and result in higher radioiodine uptake and toxicity than the sole inhibition of HDAC. The impact of such a combined therapy on *GLUT1* expression was also assessed.

RESULTS

Effects on Cell Proliferation and Cell Cycle

We had set a concentration gradient in pre-experiments. Dabrafenib at 0.1 μM and selumetinib at 2.5 μM were found to induce a preferable redifferentiation effect in BCPAP and K1 cells.[23] The half-maximum inhibitory concentrations (IC_{50}) of panobinostat in BCPAP cells, K1 cells, and BHP 2-7 cells were 62, 148, and 64 nM, respectively. MAPK inhibitor (MAPKi) (dabrafenib or selumetinib) sensitized BCPAP and K1 to dose-dependent inhibition by panobinostat. When 0.1 μM dabrafenib/2.5 μM selumetinib was added to BCPAP and K1 cells, the IC_{50} of panobinostat decreased significantly to 26/51 nM (BCPAP cells) and 21/40 nM (K1 cells), respectively; the IC_{50} of panobinostat in BHP 2-7 dropped to 59/62 nM. Therefore, panobinostat at 0.05 μM, dabrafenib at 0.1 μM, and selumetinib at 2.5 μM were used in the following experiments.

When BCPAP cells were treated with panobinostat or MAPKi (dabrafenib or selumetinib) alone for 24 h, the proportion of G1-phase cells was larger than that in the DMSO control group; when they were treated with panobinostat in combination with MAPKi (dabrafenib or selumetinib), more cells were arrested in the G1 phase than in the panobinostat alone-treated group ($p < 0.01$) (Figure 1). Results were similar in K1 cells. In BHP 2-7 cells, the number of G1 cells treated with panobinostat was larger than that in the DMSO control group, but the proportion of G1 cells in the MAPKi (dabrafenib or selumetinib)-treated BHP 2-7 cells was not significantly different from that in the DMSO control group; and the number of G1 cells in the combined treatment group was not significantly different from that in the panobinostat-treated group.

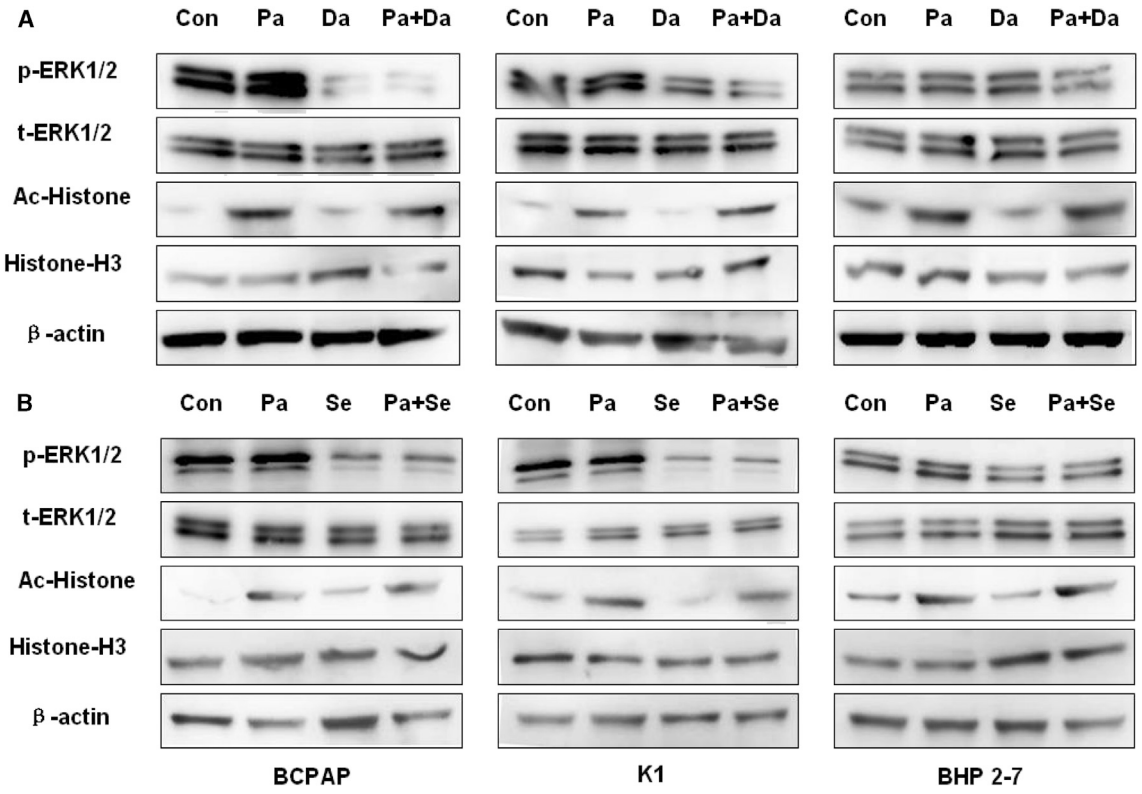

Figure 2. Western Blot of Lysates of BCPAP, K1, and BHP 2-7 Treated with 0.05 μM Panobinostat and 0.1 μM Dabrafenib/2.5 μM Selumetinib Individually or in Combination for 48 h

DMSO was used as the vehicle control. In (A), cells were treated with panobinostat and dabrafenib alone or in combination; in (B), cells were treated with panobinostat and selumetinib individually or in combination. Both panobinostat and panobinostat combined with dabrafenib/selumenitib can induce histone H3 acetylation in the three cell lines, but there was no distinct difference of global acetylation of histone H3 between HDACi alone and HDACi combined with MAPKi. In addition, they have no effect on ERK1/2 phosphorylation. Dabrafenib and selumetinib block ERK1/2 phosphorylation in BCPAP and K1, but they have no effect in BHP2-7. Besides, it has no effect on histone H3 acetylation. Con, DMSO control; Pa, panobinostat; Da, dabrafenib; Se, selumetinib.

Inhibition of the MAPK Pathway

As shown in Figure 2, treatment of cells with MAPKi (dabrafenib or selumetinib) for 48 h preferentially inhibited the phosphorylation of ERK in BCPAP and K1 cells, whereas it had no significant effect on ERK phosphorylation in BHP 2-7 cells. Panobinostat had no effect on ERK phosphorylation in all the cells.

Effect on the Acetylation Status of Histone

Panobinostat for 48 h dramatically enhanced the global acetylation of histone H3 in all the three cell lines. No effect of MAPKi (dabrafenib or selumetinib) on the global acetylation of histone H3 was found. Compared with panobinostat treatment, no enhancement of global acetylation of histone H3 was observed when MAPKi (dabrafenib or selumetinib) was added (Figure 2).

To further investigate the acetylation status of histone at the NIS gene promoter, we performed a chromatin immunoprecipitation (ChIP) assay. As shown in Figure 3, in $BRAF^{V600E}$-mutant BCPAP cells, treatment with dabrafenib resulted in a significant increase in H3K9/14 acetylation and H4K16 acetylation at the *NIS* promoter, while selumetinib increased only H4K16 acetylation at the *NIS* promoter ($p < 0.05$). Panobinostat significantly increased both H3K9/14 and H4K16 acetylation at the *NIS* promoter ($p < 0.05$). Selumetinib as well as panobinostat improved only H4K16 acetylation at the *NIS* promoter in K1 cells ($p < 0.05$). The addition of dabrafenib/selumefinib showed further increased histone acetylation at the *NIS* promoter compared with panobinostat alone in BCPAP and K1 cells ($p < 0.05$). In BHP 2-7 cells, MAPKi (dabrafenib or selumetinib) had no effect on histone acetylation at the *NIS* promoter; however, panobinostat significantly improved H3K9/14 and H4K16 acetylation. Compared with panobinostat alone, the combination with an MAPK inhibitor (MAPKi) did not further increase histone acetylation in BHP 2-7 cells.

Effect on the Expression of Iodine- and Glucose-Metabolizing Genes

In all the three PTC cells, treatment with panobinostat for 48 h increased the mRNA levels of iodine-metabolizing genes, decreased mRNA levels of *GLUT1*, but did not change the expression of *GLUT3* ($p < 0.05$) (Figure 4). After treatment with MAPKi

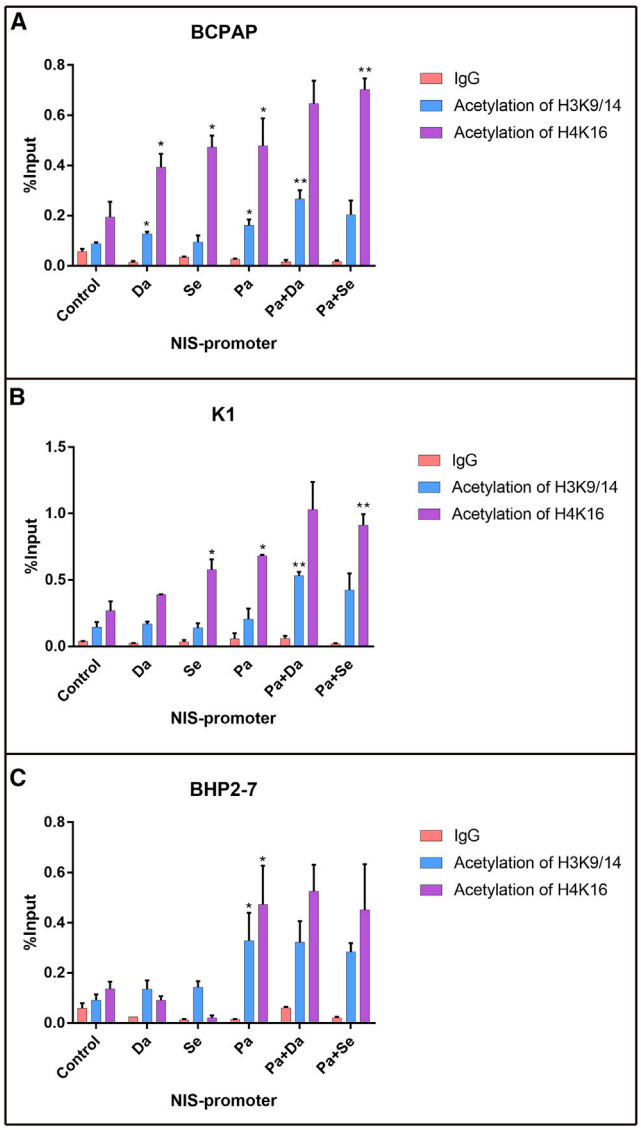

Figure 3. Effects of MAPKi or HDACi Alone or in Combination on H3K9/14 Acetylation and H4K16 Acetylation at the Human NIS Promoter in ChIP Assay

In BCPAP (A), both dabrafenib and panobinostat resulted in increasing H3K9/14 acetylation and H4K16 acetylation at the NIS promoter, while selumetinib increased only H4K16 acetylation at the NIS promoter. Selumetinib as well as panobinostat improved only H4K16 acetylation at the NIS promoter in K1 cells (B). The combination therapies showed further increased histone acetylation at the NIS promoter compared with panobinostat alone in BCPAP and K1. In BHP2-7 cells (C), MAPKi has no effect on histone acetylation at the NIS promoter, however, HDACi significantly improved H3K9/14 and H4K16 acetylation. Compared with HDACi alone, the combination with MAPKi did not further increase histone acetylation in BHP2-7. The levels of histone acetylation were expressed as fractions of the input DNA. Each bar is expressed as the mean ± SD of values. *$p < 0.05$ compared with DMSO-treated cells. **$p < 0.05$ for comparison with the panobinostat-treated group. Pa, panobinostat; Da, dabrafenib; Se, selumetinib.

(dabrafenib or selumetinib), iodine-metabolizing gene expression in BCPAP cells and K1 cells increased, *GLUT1* expression decreased ($p < 0.05$), whereas the expression of iodine- and glucose-metabolizing gene in BHP 2-7 cells did not change evidently (Figure 4). Combined treatment with panobinostat and MAPKi (dabrafenib or selumetinib) in BCPAP and K1 cells induced a higher expression level of iodine-metabolizing genes and a lower expression level of *GLUT1* than in the HDAC inhibitor (HDACi)-treated group ($p < 0.05$), whereas, in BHP 2-7 cells, mRNA levels of iodine-metabolizing genes in combined treatment groups were similar to those in the panobinostat-treated group (Figure 4).

Confocal microscopy revealed robust expression of the NIS protein when treated with HDACi (panobinostat) or MAPKi (dabrafenib or selumetinib) in BCPAP cells and K1 cells, which was even more robust when the simultaneous inhibition of HDAC and MAPK was adopted. In BHP 2-7 cells, treatment with HDACi promoted NIS protein expression, but there was no obvious difference in fluorescence intensity when combined with MAPKi (Figure 5).

Radioiodine Uptake and Efflux Assay

Compared with DMSO-treated cells, radioiodine uptake was 2.52-fold higher in BCPAP cells ($p < 0.05$), 3.16-fold higher in K1 cells ($p < 0.05$), and 3.11-fold higher in BHP 2-7 cells ($p < 0.05$) when incubated with panobinostat (Figure 6). When incubated with dabrafenib, radioiodine uptake was 1.72-fold higher in BCPAP cells and 1.64-fold higher in K1 cells compared to nontreated groups, and iodine uptake had no evident change in BHP 2-7 cells. When treated with selumetinib, radioiodine uptakes were 1.78-fold and 2.69-fold higher in BCPAP and K1 cells, respectively. However, a significant change of iodine uptake was not found in BHP 2-7 cells. Simultaneous suppression of HDAC and BRAF induced 3.73-fold and 5.03-fold higher iodine uptakes in BCPAP and K1 cells, respectively; dual suppression of HDAC and MEK induced 4.04-fold and 4.79-fold higher iodine uptakes in both $BRAF^{V600E}$-mutant cell lines.

Besides, compared with panobinostat treatment, combined therapy with MAPKi (dabrafenib or selumetinib) induced 1.62-fold ($p < 0.05$) and 1.81-fold ($p < 0.05$) higher iodine uptakes in BCPAP and 1.57-fold ($p < 0.05$) and 1.52-fold ($p < 0.05$) higher iodine uptakes in K1 cells. However, combined therapies did not significantly increase radioiodine uptake in BHP 2-7 cells.

Efflux assay showed a rapid efflux of radioactivity from the DMSO-treated BCPAP, K1, and BHP 2-7 cells, with half-lives of 6.74, 6.22, and 9.01 min, respectively. Interestingly, iodine retention was prolonged when treated with panobinostat, which could not be further strengthened when added with MAPKi (dabrafenib or selumetinib) (Figure 7).

In Vitro Clonogenic Assay

In both $BRAF^{V600E}$-mutant cell lines, the numbers of colonies decreased significantly after radioiodine treatment when pretreated with panobinostat or MAPKi (dabrafenib or selumetinib) alone

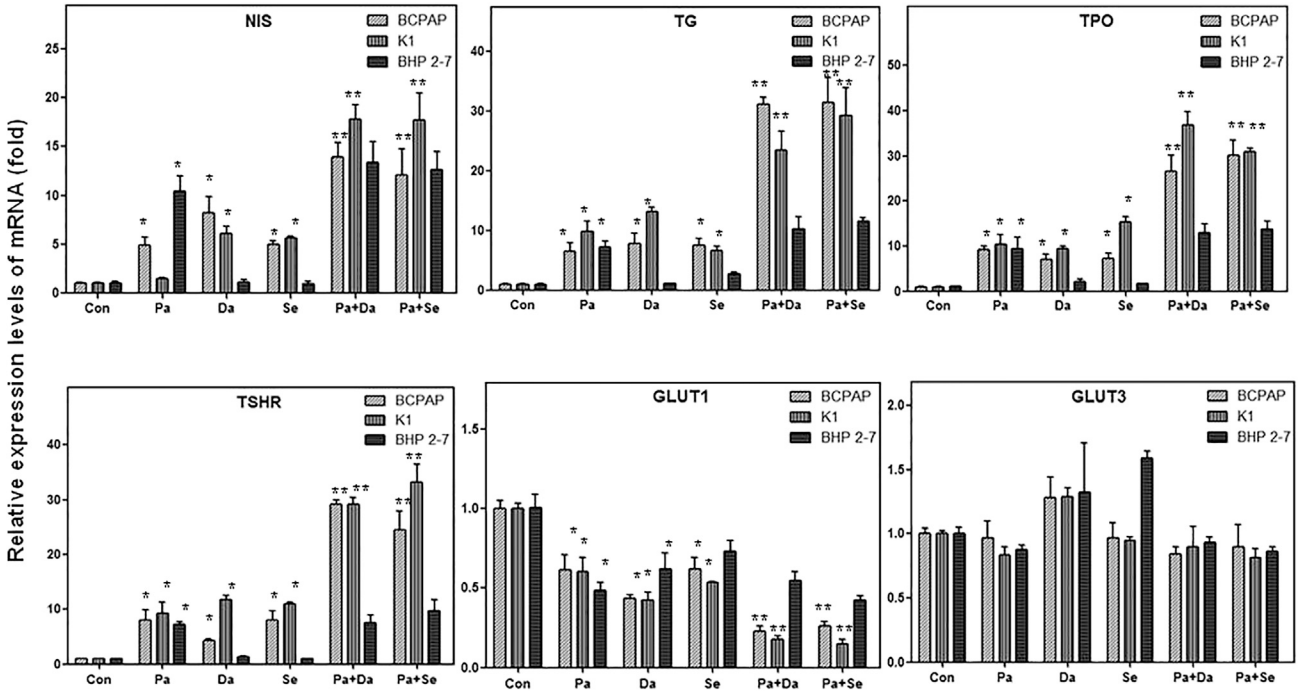

Figure 4. Effects of 0.05 μM Panobinostat and 0.1 μM Dabrafenib/2.5 μM Selumetinib, Alone or in Combination, on the mRNA Levels of *NIS*, *TG*, *TPO*, *TSHR*, and Glucose Transporter Isoform *GLUT1* and *GLUT3* Genes in BCPAP, K1, and BHP 2-7 Cells

Panobinostat for 48 h increased the mRNA levels of iodine-metabolizing genes, decreased mRNA levels of *GLUT1*, but did not change the expression of *GLUT3* in all the cells. MAPKi (dabrafenib or selumetinib) only increased iodine-metabolizing gene expression and decreased glucose-metabolizing gene expression in $BRAF^{V600E}$-mutant cells. The expression of iodine-metabolizing genes and glucose-metabolizing genes in BHP 2-7 cells was not affected by MAPKi. Combined treatment with panobinostat and MAPKi (dabrafenib or selumetinib) only induced a higher expression level of iodine-metabolizing genes and a lower expression level of *GLUT1* than the HDACi-treated group in $BRAF^{V600E}$-mutant cells, whereas, in BHP 2-7 cells, mRNA levels of iodine-metabolizing genes and glucose-metabolizing genes in combined treatment groups were similar to those in the panobinostat-treated group. Data are presented as means ± SD. *$p < 0.05$ for comparison with DMSO control. **$p < 0.05$ for comparison with the panobinostat-treated group. Con, DMSO control; Pa, panobinostat; Da, dabrafenib; Se, selumetinib.

($p < 0.05$), compared to DMSO-treated controls (Figure 8). Compared with HDACi-treated groups, the numbers of colonies further reduced when combined therapies were performed ($p < 0.05$) (Figure 8). The numbers of BHP 2-7 cell colonies were significantly reduced after radioiodine treatment when pretreated with HDACi alone ($p < 0.05$), which was not further amplified when added with MAPKi ($p > 0.05$) (Figure 8).

DISCUSSION

The silencing of *NIS*, along with other iodine-metabolizing genes, characterizes RR-DTC and results in resistance to radioiodine treatment. Since HDAC contributes to the silencing of iodine-metabolizing genes in advanced cancers, an HDACi has been considered a promising agent to induce radioiodine uptake.[24] Panobinostat is a potent pan-deacetylation inhibitor, which has previously been demonstrated to induce NIS expression in breast cancer cells and promote radioiodine uptake and sensitivity in anaplastic thyroid cancer cells.[25,26] However, although various kinds of HDACis showed a redifferentiation effect in basic research, clinical translation was not smooth. Therefore, HDACi-induced restoration of radioiodine avidity needs to be refined.

Recently, the activation of the MAPK pathway has been revealed to downregulate histone acetylation, which provides a rationale for combining MAPK pathway antagonists with HDACis to exhibit a sustained and enhanced redifferentiation effect. Dabrafenib is a BRAF inhibitor and selumetinib is an MEK inhibitor; these MAPK inhibitors have displayed a modest redifferentiation effect in PTC patients.[27] In the present study, MAPKi further enhanced HDACi-induced redifferentiation with more robust iodine-metabolizing gene expression, radioiodine uptake, and toxicity in PTC cells via simultaneously inhibiting the HDAC and MAPK pathways. Along with the previous study of Cheng et al.,[24] the improvement of HDACi-induced redifferentiation efficacy by incorporating a BRAF/MEK inhibitor in our study intensified the redifferentiation potential of the MAPKi, which provides a basis for *in vivo* and clinical studies using the combined strategy to induce more effective radioiodine therapy.

Previous studies have demonstrated that BRAF inhibitors preferentially inhibit the proliferation of PTC cells that harbor the $BRAF^{V600E}$ mutation.[28–30] Similarly, in the present study, dabrafenib showed a $BRAF^{V600E}$-dependent redifferentiation effect by preferentially

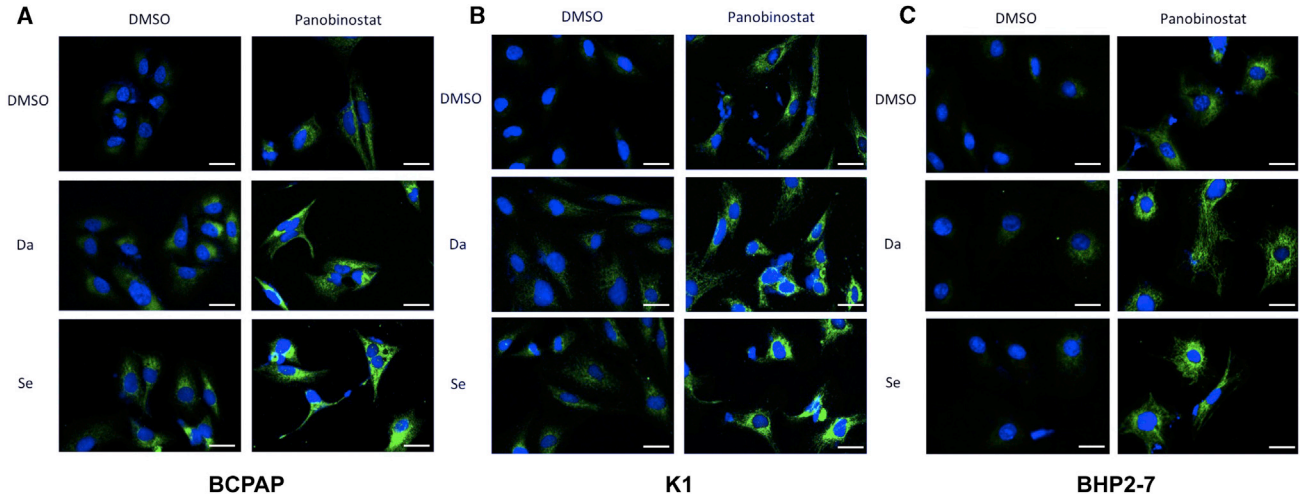

Figure 5. Confocal Microscopic Analysis of NIS Protein Expression

BRAF^{V600E}-mutant (A and B) and *BRAF*-wild-type (C) cells were treated with 0.05 μM panobinostat and 0.1 μM dabrafenib/2.5 μM selumetinib alone or in combination. The blue color represents DAPI nuclear staining and the green color represents NIS staining. NIS staining was negative in the DMSO-treated cells. NIS staining was notable in all cell lines treated with panobinostat. MAPKi (dabrafenib or selumetinib) alone only mildly enhanced NIS expression in BCPAP and K1, but it was invalid in BHP 2-7. Compared with the NIS expression of panobinostat-alone treatment, more robust expression of NIS was only seen in *BRAF*^{V600E}-mutant cells when panobinostat and MAPKi (dabrafenib or selumetinib) were used in combination. Scale bars represent 25 μm in all panels. Da, dabrafenib; Se, selumetinib.

suppressing MAPK signaling, inhibiting cell proliferation, arresting cell cycle, and regulating iodine- and glucose-metabolizing gene expression in *BRAF*^{V600E}-positive PTC cells. The MEK inhibitor selumetinib also showed a redifferentiation effect in a *BRAF*^{V600E}-dependent manner, but it had no significant effect in *BRAF* wide-type BHP 2-7 cells. The underlying mechanism of HDACi-induced upregulation of *NIS* gene expression via improving the acetylation status of histone at the promoter was elucidated directly by ChIP assay in our study. Moreover, compared with *BRAF*-wild-type cells, MAPKi further increased the HDACi-induced acetylation of histone at the *NIS* promoter in *BRAF*^{V600E}-mutant cells, indicating a *BRAF*^{V600E}-dependent redifferentiation effect of MAPKi. Such novel findings may lead to a precisely improved redifferentiation strategy of RR-DTC.

It is well known that the differentiation status of tumor cells can also be quantitatively reflected by glucose metabolism activity, which makes ^{18}F-FDG PET very useful in evaluating the biochemical behavior of tumors. To the opposite of iodide-handling genes, glucose-metabolizing genes have been recognized to inversely correlate with the differentiation status of thyroid cancer. Radioiodine non-avid thyroid cancer lesions tend to be FDG avid due to intense glucose uptake and metabolism.[17] A molecular mechanism underlying increased FDG uptake in RR-DTC is that dedifferentiation in thyroid cancer is accompanied by *GLUT1* upregulation.[7,8] In the present study, the expression levels of *GLUT1* in PTC cells decreased significantly after the inhibition of HDAC or BRAF/MEK, and they were even lower after the dual suppression of both HDAC and BRAF/MEK, further demonstrating the improvement of the HDACi-induced differentiation effect, via adding the BRAF/MEK inhibitor, and providing a rationale for monitoring redifferentiation efficacy using ^{18}F-FDG PET. *GLUT3* expression level was not significantly changed in the present study, which is consistent with Perrier's findings.[31]

It is worthy of mentioning that the sufficient retention of radioiodine in tumors is one of the most important prerequisites for adequate radiation dose, which involves two steps of transport by cells, basolateral uptake and apical efflux.[32] While iodine uptake is generated by the NIS presenting in the basolateral plasma membrane, efflux of iodine across the apical membrane is mediated by pendrin, *SLC5A8*, and *ClCn5*.[33–35] Interestingly, the radioiodine efflux assay in our study showed that panobinostat alone prolonged iodine retention in all the cells, which is similar to its effect on anaplastic thyroid cancer (ATC) cells in previous study.[26] However, compared with HDACi treatment, the addition of MAPKi (dabrafenib or selumetinib) did not further prolong radioiodine retention in all the PTC cells. It seems that MAPK inhibitors, unlike HDACis, may not affect the activity of apical membrane proteins. Actually, *in vivo* iodide anion not organized by TPO undergoes rapid efflux from follicular thyroid cells. Thus, a balance between NIS-mediated iodide uptake and TPO-inhibited efflux determines the intracellular concentration and radiation dose of radioiodine.[35] In addition, that the retention time could not be further strengthened by combined therapies may also be explained by the inappropriate time window, which has been reflected by the differing redifferentiation efficacy of MAPKi between preclinical experiments and clinical trial.[6]

In conclusion, this study demonstrated that MAPKi enhances HDACi-induced redifferentiation efficacy in PTC cells harboring

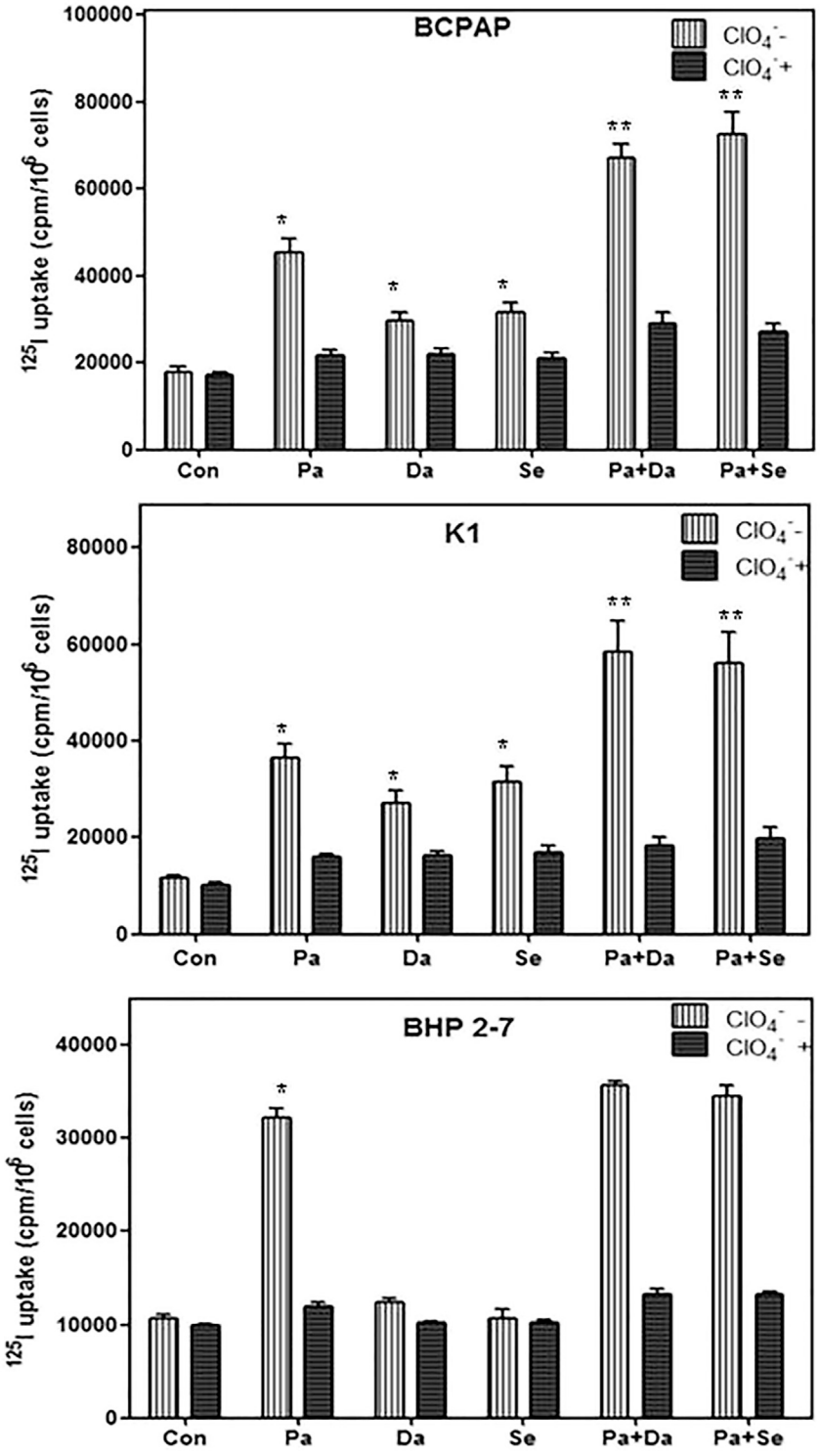

Figure 6. Radioactive Iodine Uptake in BCPAP Cells, K1 Cells, and BHP 2-7 Cells

Cells were treated with 0.05 μM panobinostat and 0.1 μM dabrafenib/2.5 μM selumetinib alone or in combination. HDACi increased the radioactive iodine uptake in all the cells, whereas MAPKi only enhanced radioactive iodine uptake in *BRAF*^{V600E}-mutant cells. The addition of MAPKi further strengthened radioactive iodine uptake in *BRAF*^{V600E}-mutant cells compared with HDACi alone, whereas combined therapies had no effect in *BRAF*-wild-type cells. Data are expressed as mean ± SD of values. *$p < 0.05$ compared with DMSO-treated cells. **$p < 0.05$ for comparison with the panobinostat-treated group. Con, DMSO control; Pa, panobinostat; Da, dabrafenib; Se, selumetinib.

BRAF^{V600E}. It provides a basis for *in vivo* and clinical studies using both HDACi and MAPKi as adjuvant agents in radioiodine therapy, which may be translated to a potential therapeutic strategy for RR-DTC.

MATERIALS AND METHODS

Cell Culture and Agents

The HDACi (panobinostat) and MAPK inhibitor (MAPKi, dabrafenib and selumetinib) (Medchem Express [MCE]) were made up to a stock solution of 10 mM in DMSO.

Three PTC cell lines were utilized in this study. The BCPAP cell line was purchased from the Chinese Academy of Science, and the K1 cell line was obtained from the Health Protection Agency culture collection. The BHP 2-7 cell line was kindly provided by the Division of Endocrinology, David Geffen School of Medicine, University of California, Los Angeles. They were all maintained at 37°C with 5% CO_2 in RPMI 1640 medium supplemented with 10% fetal bovine serum (FBS). All cell lines are authenticated for correct origin by short tandem repeat (STR) analysis. The passage of the cells at which the following evaluations had been performed is 10–20.

Oncogene Analysis and Cell Proliferation Assay

Total RNA was prepared from the cells for oncogene analysis using an RNeasy kit (QIAGEN). Mutant *BRAF*^{V600E} and wild-type *NRAS* genes were confirmed in BCPAP and K1 cells. *RET/PTC1* rearrangement, wild-type genes of *BRAF* and *NRAS*, were confirmed in BHP 2-7 cells, as previously described by our team.[23]

After cells were cultured with increasing concentrations of panobinostat and MAPKi (dabrafenib or selumetinib) alone or in combination for 24, 48, and 72 h, the Cell Counting Kit-8 (Dojindo Molecular Technologies) was used to detect cell proliferation. IC_{50} was calculated using GraphPad Prism 5.0.

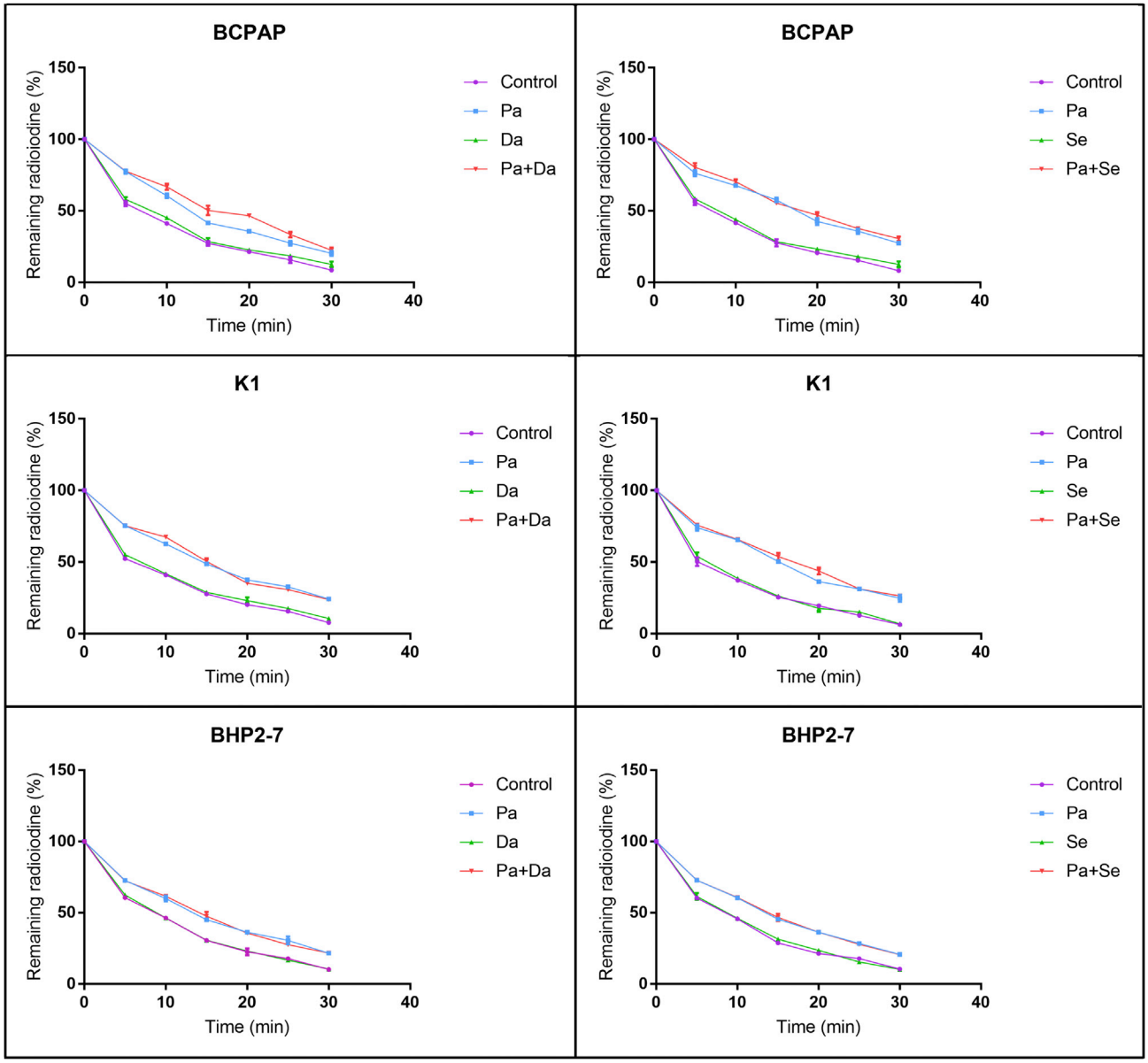

Figure 7. Radioactive Iodine Efflux in BCPAP Cells, K1 Cells, and BHP 2-7 Cells

Cells were treated with 0.05 μM panobinostat and 0.1 μM dabrafenib/2.5 μM selumetinib alone or in combination. Panobinostat prolonged the retention time of radioactive iodine in all the cells. MAPKi (dabrafenib or selumetinib) had no effect in all the cells. Panobinostat combined with MAPKi (dabrafenib or selumetinib) did not further prolong retention time compared with panobinostat alone in all the cells. Data are expressed as mean ± SD. Con, DMSO control; Pa, panobinostat; Da, dabrafenib; Se, selumetinib.

Cell Cycle Analysis

Cells (3.0×10^5) were grown in 25-cm^2 flasks overnight and incubated with panobinostat and MAPKi (dabrafenib or selumetinib) alone, in combination, or with DMSO for 24 h. Cells were fixed, washed, and resuspended in PBS containing 1.0 mg/mL RNase A and 1.0 mg/mL propidium iodide. Propidium iodide-stained cells were analyzed by flow cytometry (Becton Dickinson, USA).

RNA Extraction and Real-Time qRT-PCR Analysis

Cells (3.0×10^5) were seeded in 25-cm^2 flasks and then treated with panobinostat and MAPKi (dabrafenib or selumetinib) individually, in combination, or with DMSO. After 48 h of treatment, total RNA was extracted using an RNeasy kit (QIAGEN), Total RNA (1 μg) was converted to cDNA on an iCycler Thermal Cycler (Bio-Rad) using a QuantiTect Reverse Transcription Kit (QIAGEN). Real-time qRT-PCR analysis was performed to evaluate the expression of

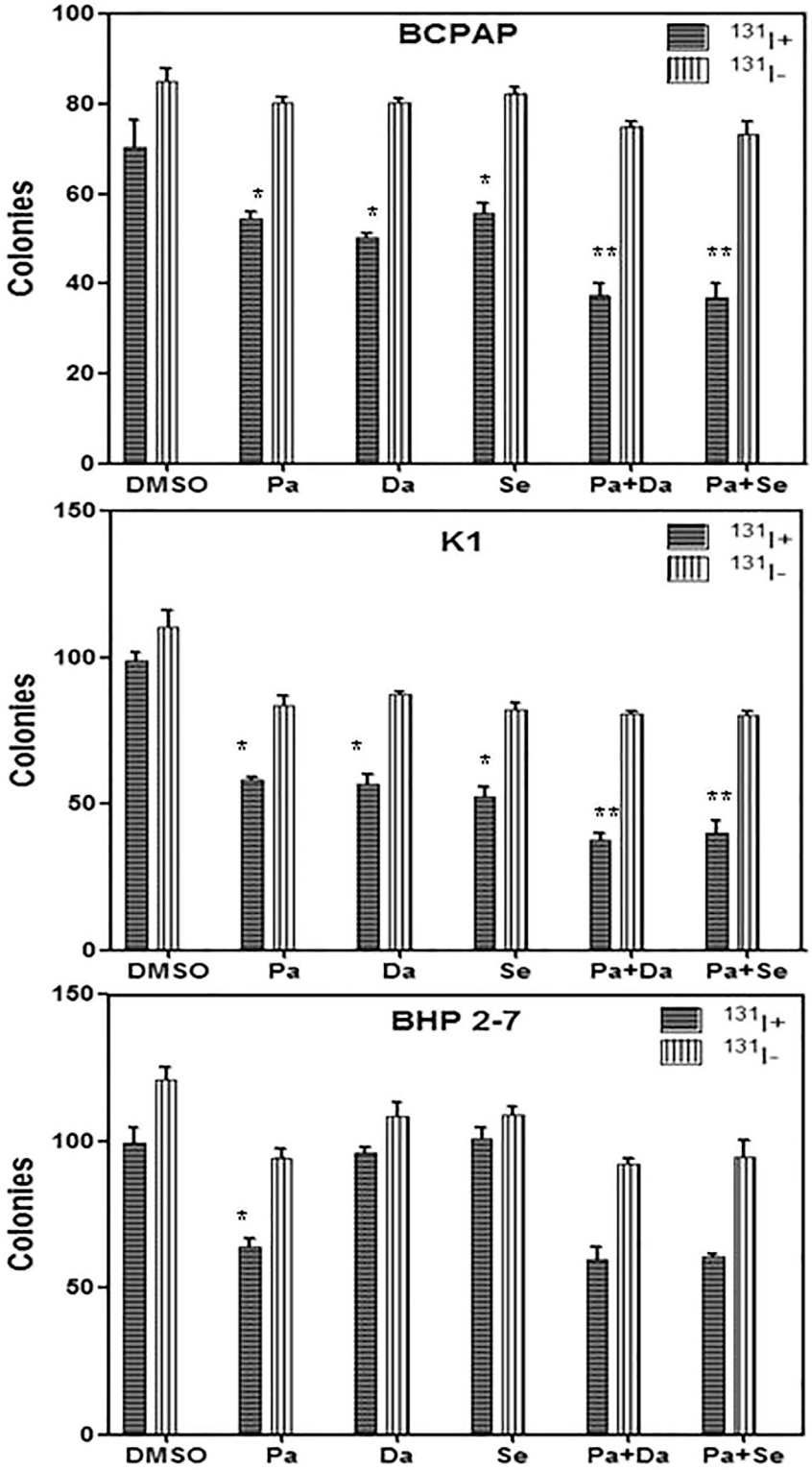

Figure 8. *In Vitro* Clonogenic Assay

Data are represented as number of colonies in BCPAP cells, K1 cells, and BHP 2-7 cells treated with 0.05 μM panobinostat and 0.1 μM dabrafenib/2.5 μM selumetinib alone or in combination with (^{131}I+) or without (^{131}I–) ^{131}I. The numbers of colonies in *BRAF*^{V600E}-mutant cells decreased significantly after radioiodine treatment when pretreated with panobinostat or MAPKi (dabrafenib or selumetinib) compared to DMSO-treated controls. Compared with HDACi-treated groups, the numbers of colonies further reduced in *BRAF*^{V600E}-mutant cells when combined therapies were performed. The numbers of BHP 2-7 cell colonies were significantly reduced after radioiodine treatment when pretreated with HDAC inhibitor alone, which were not further amplified when added with MAPKi. Data are expressed as mean ± SD. *$p < 0.05$ compared with DMSO-treated cells. **$p < 0.05$ for comparison with the panobinostat-treated group. Pa, panobinostat; Da, dabrafenib; Se, selumetinib.

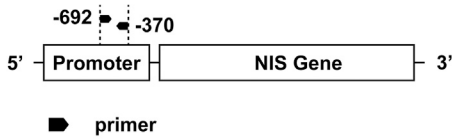

Figure 9. The Schematic Diagram of the Primer Locations Relative to the NIS Gene Promoter and Gene Body
The amplicon size is 323 bp (−629/−370).

thyroid genes on an ABI Prism 7900HT Sequence Detector (Applied Biosystems), using SYBR Green MasterMix (QIAGEN). The expression value of each gene (*NIS*, *TSHR*, *TG*, *TPO*, *GLUT1*, and *GLUT3*) was normalized to 18S cDNA to calculate the relative amount of RNA present in each sample.[17]

Western Blotting Assay

Cells were lysed in radio immunoprecipitation assay (RIPA) buffer. Equal amounts of total protein were separated on 6%, 8%, and 12% SDS-PAGE and transferred onto polyvinylidene difluoride membranes (Millipore). The membranes were then probed with the following primary antibodies: p-Erk1/2, Erk1/2, Ac-Histone H3, and Histone H3 (Cell Signaling Technology); and β-actin, 1:5,000 (Protein Tech). Membranes were then incubated with species-specific horseradish peroxidase (HRP)-conjugated antibodies. Protein bands in the membrane were visualized with ECL reaction reagents (Beyotime).

Immunofluorescent Localization of NIS

Cells (2.0×10^4) were seeded in 6-well chamber slides. After 72 h of treatment with specific inhibitors, cells were fixed in 4% paraformaldehyde and blocked with 1% BSA. Cells were then incubated in succession with rabbit anti-NIS diluted at 1:100 (Protein Tech), Alexa Fluor 488-conjugated Goat anti-rabbit immunoglobulin G (IgG) secondary antibody diluted at 1:100 (Thermo Fisher Scientific), and DAPI. Confocal microscopy examination (Leica SP8, German) was performed to monitor NIS expression.

Iodine Uptake and Efflux Assay

Cells (1.5×10^5) were seeded in 6-well plates and then incubated with panobinostat and MAPKi (dabrafenib or selumetinib) individually, in combination, or with DMSO for 48 h. Iodide uptake and iodine efflux assays were performed as previously described by our team.[36]

Radioiodine Cytotoxicity Assay

Radioiodine cytotoxicity was performed as previously reported by our group with minor modification.[36] Cells (4×10^2) were seeded in 6-well plates and left 48 h to attach. 48 h after treatment with specific drugs, medium was discarded and cells were washed twice in PBS. The medium was then replaced with 1 mL RPMI 1640 in the presence or absence of 20 μCi $Na^{131}I$ for 6 h. At the end of the treatment, the radioactive medium was discarded, and cells were washed and left in regular culture medium for 7 days. Finally, cells were fixed in methanol and stained with crystal violet, and the number of colonies was counted.

Table 1. qPCR Primer of the *NIS* Promoter for ChIP Studies

	Primer Sequences (5′-3′)	Amplicon Size (bp) and Nucleotide Number
NIS promoter	forward GAGTGCTGAAGCAGGCTGTGC	323 (−692/−370)
	reverse GGGAGCAGCTCGTGATTGTGG	

ChIP Assay

ChIP assay was performed with the EZ-Magna ChIP A kit (17-408, Millipore), according to the manufacturer's protocol. Briefly, protein and DNA was crosslinked by incubating cells with 37% fromaldehyde followed by quenching unreacted formaldehyde with glycine. Chromatin was sheared to lengths between 200 and 1,000 bp with sonication (Bioruptor, Diagenode), followed by incubation overnight at 4°C with anti-histone acetylation antibodies, including anti-acetylated H3K9/14 (06-599B, Millipore), anti-acetylated H4K16 (17-10101, Millipore), normal rabbit IgG (PP64B), and fully suspended protein A magnetic beads. Crosslinks of protein and DNA complexes were reversed by incubating with proteinase K at 62°C for 2 h with shaking after washing protein A beads-antibody and chromatin complexes with 500 μL washing buffer. Spin columns were used for DNA purifying. Human *NIS* primer corresponding to the defined region of the *NIS* promoter (Figure 9; Table 1) was used to perform real-time qPCR to detect DNA fragments obtained from ChIP.[22]

Statistical Analysis

All the experiments were done three times. The data on cell cycle assay were analyzed using the chi-square test. The remaining data on RT-PCR, ChIP, radioiodine uptake and efflux, and toxicity assays were analyzed using the independent-samples t test. All statistical analyses were performed using SPSS version 17.0. Significance was set as $p < 0.05$.

AUTHOR CONTRIBUTIONS

H.F. and Lingxiao Cheng conducted the experiments and wrote the paper. Y.J., Lin Cheng, and M.L. worked on figures and edited the manuscript. L.C. conceived the idea, designed the experiments, and gave final approval of the version to be published.

CONFLICTS OF INTEREST

We declare that all the authors have read and approved the final draft of the manuscript for submission, and there are no conflicts of interest to declare.

ACKNOWLEDGMENTS

This work was supported by the National Natural Science Foundation of China (81671711 and 81701731). We thank Dr. Weibin Wang from Zhejiang University School of Medicine for helpful discussion.

REFERENCES

1. Reiners, C., Hänscheid, H., Luster, M., Lassmann, M., and Verburg, F.A. (2011). Radioiodine for remnant ablation and therapy of metastatic disease. Nat. Rev. Endocrinol. *7*, 589–595.

2. Cheng, L., Liu, M., Ruan, M., and Chen, L. (2016). Challenges and strategies on radioiodine treatment for differentiated thyroid carcinoma. Hell. J. Nucl. Med. *19*, 23–32.
3. Jin, Y., Van Nostrand, D., Cheng, L., Liu, M., and Chen, L. (2018). Radioiodine refractory differentiated thyroid cancer. Crit. Rev. Oncol. Hematol. *125*, 111–120.
4. Scott, E., Learoyd, D., and Clifton-Bligh, R.J. (2016). Therapeutic options in papillary thyroid carcinoma: current guidelines and future perspectives. Future Oncol. *12*, 2603–2613.
5. Vaisman, F., Carvalho, D.P., and Vaisman, M. (2015). A new appraisal of iodine refractory thyroid cancer. Endocr. Relat. Cancer *22*, R301–R310.
6. Kreissl, M.C., Janssen, M.J.R., and Nagarajah, J. (2019). Current treatment strategies in metastasized differentiated thyroid cancer. J. Nucl. Med. *60*, 9–15.
7. Kim, S., Chung, J.K., Min, H.S., Kang, J.H., Park, D.J., Jeong, J.M., Lee, D.S., Park, S.H., Cho, B.Y., Lee, S., and Lee, M.C. (2014). Expression patterns of glucose transporter-1 gene and thyroid specific genes in human papillary thyroid carcinoma. Nucl. Med. Mol. Imaging *48*, 91–97.
8. Grabellus, F., Nagarajah, J., Bockisch, A., Schmid, K.W., and Sheu, S.Y. (2012). Glucose transporter 1 expression, tumor proliferation, and iodine/glucose uptake in thyroid cancer with emphasis on poorly differentiated thyroid carcinoma. Clin. Nucl. Med. *37*, 121–127.
9. Annunziato, A.T., and Hansen, J.C. (2000). Role of histone acetylation in the assembly and modulation of chromatin structures. Gene Expr. *9*, 37–61.
10. Hou, P., Bojdani, E., and Xing, M. (2010). Induction of thyroid gene expression and radioiodine uptake in thyroid cancer cells by targeting major signaling pathways. J. Clin. Endocrinol. Metab. *95*, 820–828.
11. Furuya, F., Shimura, H., Suzuki, H., Taki, K., Ohta, K., Haraguchi, K., Onaya, T., Endo, T., and Kobayashi, T. (2004). Histone deacetylase inhibitors restore radioiodide uptake and retention in poorly differentiated and anaplastic thyroid cancer cells by expression of the sodium/iodide symporter thyroperoxidase and thyroglobulin. Endocrinology *145*, 2865–2875.
12. Liu, D., Hu, S., Hou, P., Jiang, D., Condouris, S., and Xing, M. (2007). Suppression of BRAF/MEK/MAP kinase pathway restores expression of iodide-metabolizing genes in thyroid cells expressing the V600E BRAF mutant. Clin. Cancer Res. *13*, 1341–1349.
13. Hou, P., Liu, D., Ji, M., Liu, Z., Engles, J.M., Wahl, R.L., and Xing, M. (2009). Induction of thyroid gene expression and radioiodine uptake in melanoma cells: novel therapeutic implications. PLoS ONE *4*, e6200.
14. Amoêdo, N.D., Rodrigues, M.F., Pezzuto, P., Galina, A., da Costa, R.M., de Almeida, F.C., El-Bacha, T., and Rumjanek, F.D. (2011). Energy metabolism in H460 lung cancer cells: effects of histone deacetylase inhibitors. PLoS ONE *6*, e22264.
15. Woyach, J.A., Kloos, R.T., Ringel, M.D., Arbogast, D., Collamore, M., Zwiebel, J.A., Grever, M., Villalona-Calero, M., and Shah, M.H. (2009). Lack of therapeutic effect of the histone deacetylase inhibitor vorinostat in patients with metastatic radioiodine-refractory thyroid carcinoma. J. Clin. Endocrinol. Metab. *94*, 164–170.
16. Sherman, E.J., Su, Y.B., Lyall, A., Schöder, H., Fury, M.G., Ghossein, R.A., Haque, S., Lisa, D., Shaha, A.R., Tuttle, R.M., and Pfister, D.G. (2013). Evaluation of romidepsin for clinical activity and radioactive iodine reuptake in radioactive iodine-refractory thyroid carcinoma. Thyroid *23*, 593–599.
17. Ruan, M., Liu, M., Dong, Q., and Chen, L. (2015). Iodide- and glucose-handling gene expression regulated by sorafenib or cabozantinib in papillary thyroid cancer. J. Clin. Endocrinol. Metab. *100*, 1771–1779.
18. Chakravarty, D., Santos, E., Ryder, M., Knauf, J.A., Liao, X.H., West, B.L., Bollag, G., Kolesnick, R., Thin, T.H., Rosen, N., et al. (2011). Small-molecule MAPK inhibitors restore radioiodine incorporation in mouse thyroid cancers with conditional BRAF activation. J. Clin. Invest. *121*, 4700–4711.
19. Hoftijzer, H., Heemstra, K.A., Morreau, H., Stokkel, M.P., Corssmit, E.P., Gelderblom, H., Weijers, K., Pereira, A.M., Huijberts, M., Kapiteijn, E., et al. (2009). Beneficial effects of sorafenib on tumor progression, but not on radioiodine uptake, in patients with differentiated thyroid carcinoma. Eur. J. Endocrinol. *161*, 923–931.
20. Ho, A.L., Grewal, R.K., Leboeuf, R., Sherman, E.J., Pfister, D.G., Deandreis, D., Pentlow, K.S., Zanzonico, P.B., Haque, S., Gavane, S., et al. (2013). Selumetinib-enhanced radioiodine uptake in advanced thyroid cancer. N. Engl. J. Med. *368*, 623–632.
21. Rothenberg, S.M., Daniels, G.H., and Wirth, L.J. (2015). Redifferentiation of Iodine-Refractory BRAF V600E-Mutant Metastatic Papillary Thyroid Cancer with Dabrafenib-Response. Clin. Cancer Res. *21*, 5640–5641.
22. Zhang, Z., Liu, D., Murugan, A.K., Liu, Z., and Xing, M. (2014). Histone deacetylation of NIS promoter underlies BRAF V600E-promoted NIS silencing in thyroid cancer. Endocr. Relat. Cancer *21*, 161–173.
23. Cheng, L., Jin, Y., Liu, M., Ruan, M., and Chen, L. (2017). HER inhibitor promotes BRAF/MEK inhibitor-induced redifferentiation in papillary thyroid cancer harboring BRAFV600E. Oncotarget *8*, 19843–19854.
24. Cheng, W., Liu, R., Zhu, G., Wang, H., and Xing, M. (2016). Robust Thyroid Gene Expression and Radioiodine Uptake Induced by Simultaneous Suppression of BRAF V600E and Histone Deacetylase in Thyroid Cancer Cells. J. Clin. Endocrinol. Metab. *101*, 962–971.
25. Fortunati, N., Catalano, M.G., Marano, F., Mugoni, V., Pugliese, M., Bosco, O., Mainini, F., and Boccuzzi, G. (2010). The pan-DAC inhibitor LBH589 is a multifunctional agent in breast cancer cells: cytotoxic drug and inducer of sodium-iodide symporter (NIS). Breast Cancer Res. Treat. *124*, 667–675.
26. Pugliese, M., Fortunati, N., Germano, A., Asioli, S., Marano, F., Palestini, N., Frairia, R., Boccuzzi, G., and Catalano, M.G. (2013). Histone deacetylase inhibition affects sodium iodide symporter expression and induces 131I cytotoxicity in anaplastic thyroid cancer cells. Thyroid *23*, 838–846.
27. Fröhlich, E., and Wahl, R. (2014). The current role of targeted therapies to induce radioiodine uptake in thyroid cancer. Cancer Treat. Rev. *40*, 665–674.
28. Salerno, P., De Falco, V., Tamburrino, A., Nappi, T.C., Vecchio, G., Schweppe, R.E., Bollag, G., Santoro, M., and Salvatore, G. (2010). Cytostatic activity of adenosine triphosphate-competitive kinase inhibitors in BRAF mutant thyroid carcinoma cells. J. Clin. Endocrinol. Metab. *95*, 450–455.
29. Rothenberg, S.M., McFadden, D.G., Palmer, E.L., Daniels, G.H., and Wirth, L.J. (2015). Redifferentiation of iodine-refractory BRAF V600E-mutant metastatic papillary thyroid cancer with dabrafenib. Clin. Cancer Res. *21*, 1028–1035.
30. Matsuzu, K., Segade, F., Matsuzu, U., Carter, A., Bowden, D.W., and Perrier, N.D. (2004). Differential expression of glucose transporters in normal and pathologic thyroid tissue. Thyroid *14*, 806–812.
31. Pesce, L., Bizhanova, A., Caraballo, J.C., Westphal, W., Butti, M.L., Comellas, A., and Kopp, P. (2012). TSH regulates pendrin membrane abundance and enhances iodide efflux in thyroid cells. Endocrinology *153*, 512–521.
32. Rodriguez, A.M., Perron, B., Lacroix, L., Caillou, B., Leblanc, G., Schlumberger, M., Bidart, J.M., and Pourcher, T. (2002). Identification and characterization of a putative human iodide transporter located at the apical membrane of thyrocytes. J. Clin. Endocrinol. Metab. *87*, 3500–3503.
33. van den Hove, M.F., Croizet-Berger, K., Jouret, F., Guggino, S.E., Guggino, W.B., Devuyst, O., and Courtoy, P.J. (2006). The loss of the chloride channel, ClC-5, delays apical iodide efflux and induces a euthyroid goiter in the mouse thyroid gland. Endocrinology *147*, 1287–1296.
34. Mu, D., Huang, R., Ma, X., Li, S., and Kuang, A. (2012). Radioiodine therapy of thyroid carcinoma following Pax-8 gene transfer. Gene Ther. *19*, 435–442.
35. Chen, L., Altmann, A., Mier, W., Eskerski, H., Leotta, K., Guo, L., Zhu, R., and Haberkorn, U. (2006). Radioiodine therapy of hepatoma using targeted transfer of the human sodium/iodide symporter gene. J. Nucl. Med. *47*, 854–862.
36. Xing, J., Liu, R., Xing, M., and Trink, B. (2011). The BRAFT1799A mutation confers sensitivity of thyroid cancer cells to the BRAFV600E inhibitor PLX4032 (RG7204). Biochem. Biophys. Res. Commun. *404*, 958–962.